All-optical demultiplexing using an electroabsorption modulator

Højfeldt, Sune; Bischoff, Svend; Mørk, Jesper

Published in:
Proceedings of Lasers and Electro-Optics

Link to article, DOI:
10.1109/CLEO.2000.907091

Publication date:
2000

Document Version
Publisher's PDF, also known as Version of record

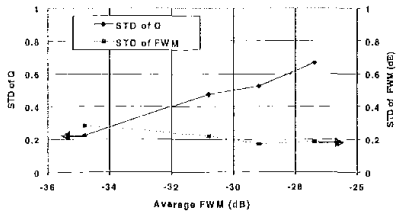

CWK69 Fig. 2. Measured standard deviations of Q as a function of average FWM crosstalk.

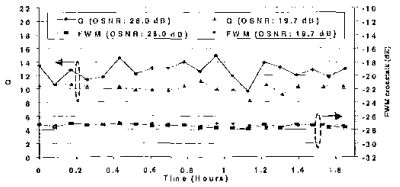

CWK69 Fig. 3. Measured Q values for different OSNR in 1.7 hours.

for case (b). Also no obvious correlation between the FWM crosstalk variations and Q fluctuations was observed. Fig. 2 gives the standard deviations (STD) of measured Q as a function of the average FWM crosstalk. It shows that the magnitudes of fluctuations of Q values increase as FWM crosstalk increases, while the standard deviation of FWM crosstalk decreases slowly with the increase of the average FWM crosstalk. Therefore, the fluctuations of Q values are not correlated to the variations of FWM crosstalk level.

To further evaluate the Q variations, we measured Q values for different OSNR. Fig. 3 shows measured Q values in about 1.7 hours for two OSNRs, 19.7 dB and 28.0 dB. The average FWM crosstalk level was unchanged for these two cases. From Fig. 3, we observe that increasing amplified spontaneous emission (decreasing OSNR) reduces not only the magnitude of Q, but also the fluctuation of Q. This is contrary to the FWM effect which reduces the magnitude of Q, but increase its fluctuations, as shown in Fig. 2.

From our measurement results, we believe that the Q fluctuations were related to FWM, but not induced by the variations of FWM crosstalk level. The causes of the Q fluctuation can be tracked in two directions. First, part of fluctuations may simply come from the accuracy reduction of the Q measurement method due to the non-Gaussian statistics of FWM crosstalk, which increases the difficulty to get a good fitting curve from the measured points and induces large fluctuations among different measurements even though the system performance might be quite stable. This can be justified by the fact that decreasing OSNR reduces the Q fluctuations, as shown in Fig. 3.

The second reason of the Q variations goes to the real system performance fluctuations. Though the FWM crosstalk varies little, but its phase may vary due to the laser frequency shifts and the variations of fiber characteristics. Thus the FWM degradation on the channel signals may vary since the interference effect of FWM on the channel signal depends on the phase. We would expect the same from polarization states, since the interference effect of FWM also depends on the polarization states of the channel signals and the FWM signals. However, we know that polarization variations should also induce fluctuations on FWM crosstalk.[7] But, as shown in Fig. 2 and Fig. 3, no large fluctuations were observed on FWM crosstalk. Therefore, there should be no large polarization effect on the variations of system performance. The phase fluctuation is the main factor for the system performance fluctuations. This can be partly justified by the fact that measured Q values drifted from time to time and also the magnitudes of the drifts are highly related to the levels of average FWM crosstalk.

In summary, we have investigated FWM induced Q fluctuations in WDM systems. Our measured results show that FWM can induce large variations on system Q-factor. The magnitudes of the fluctuation on Q have little correlation to the magnitudes of fluctuations of FWM power, but strongly depend on the average FWM crosstalk level. We believe that these fluctuations mainly result from FWM induced non-Gaussian characteristics of the noise in channel signals and also from the variations of the phase coherency between the FWM signals and the channel signals. Thus, these fluctuations may have great impacts on the performance of forward-error correction (FEC) that will be implemented widely in next generation WDM systems.

1. S. Song, *et al.*, "Experimental study of four-wave mixing in non-zero dispersion fiber," Proc. of LEOS'97, WAA2, pp. 224–225, Nov. 1997.
2. S. Song, *et al.*, "Higher-order four-wave mixing and its effects in WDM systems," submitted to CLEO2000, San Francisco, CA, May, 2000.
3. N.S. Bargano, *et al.*, "320 Gb/s WDM transmission (64 × 5 Gb/s) over 7,200 km using large mode fiber spans and chirped return-to-zero signals," OFC'98, PD12, San Jose, Feb. 1998.
4. H. Taga, *et al.*, "The first demonstration of four-channel simultaneous performance measurement of long distance WDM transmission systems," Proc. of ECOC'99, Vol. II, pp. 188–189, Nice, France, Sept. 1999.
5. K. Inoue, H. Toba, "Fiber four-wave mixing in multi-amplifier systems with non-uniform chromatic dispersion," J. of Lightwave Technology, **13** (1) 89–93 (Jan. 1995).
6. S. Song, *et al.*, "Intensity dependent effects on four-wave mixing in optical fiber," J. of Lightwave Technology, **17** (11) 2285–2290 (Nov. 1999).
7. S. Song, *et al.*, "A novel nonlinear method for measuring polarization mode dispersion using four-wave mixing," To be published in J. of Lightwave Technology, **17** (12) (1999).
8. N.S. Bargano, *et al.*, "Margin measurements in optical amplifier systems," IEEE Photonics Letts. **5** (3) 304–306 (1993).

CWK70

All-optical demultiplexing using an electroabsorption modulator

S. Højfeldt, S. Bischoff, J. Mørk, *Res. Ctr. COM, Technical Univ. of Denmark, Bldg. 344, DK-2800, Lyngby, Denmark; E-mail: sh@com.dtu.dk*

In the last decade, the electroabsorption modulator (EAM) has found a wide range of applications. Functionalities such as pulse generation and demultiplexing by electrical modulation[1] have been demonstrated using an EAM. Recently, all-optical wavelength conversion,[2,3] demultiplexing,[4] and signal regeneration,[5] have also been experimentally demonstrated. In this paper, we investigate all-optical demultiplexing from 80 to 10 Gbit/s.

Our model for a reverse-biased quantum-well absorber is a large-signal model developed for studying all-optical wavelength conversion and signal regeneration.[6] The absorption recovery of the device is governed by the sweep-out of photogenerated carriers. Based on the experimental results in[4] we take the sweep-out time to be 8 ps.

Figure 1 shows the demultiplexing configuration. An incoming 80-Gbit/s-signal at 1510 nm and a 10-Gbit/s control signal at 1520 nm are launched into an EAM (band-gap at 1550 nm). Through cross-absorption saturation, the control signal gates the desired channel. To investigate the demultiplexing capability of the EAM, we propagate various 80-Gbit/s bit-patterns through the device together with a 10-Gbit/s control signal. Both consist of 3 ps wide pulses. The incoming signal had an extinction ratio (*ER*) of 10 dB (peak-to-floor), introduced to simulate noise in the signal. The control signal had an *ER* of 20 dB.

Figure 2 shows the eye-diagrams as function of device length. The figure shows that at $L = 85$ μm, the channels to be rejected are still quite strong. At $L = 125$ μm, the rejected channels are suppressed ~9 dB. In the eye for the 125 μm long device, a gated space is responsible for one of the strong remaining pulses. Due to the combined effects of absorption saturation, and the finite sweep-out time, a gated space can experience a smaller absorption than a gated mark. This is an intrinsic property of this type of demultiplexing scheme used at high bit-rates (compared to the sweep-out time), and hence the maximum obtainable level of rejection at the output is very similar to the input stream *ER* (here: 10 dB), but lower. For simple demultiplexing, the device is simple and useful, but cannot compete with e.g. the Mach-Zehnder interferometer in drop-functionality because there is no signal improvement.

Figure 3 shows the suppression of the rejected channels compared to the demultiplexed channel as function of device length for different control pulse powers. As expected, higher control pulse power gives better rejection of neighboring channels. For each power level, the level-of-rejection increases up to a certain device length, beyond which the output power just decreases, thereby identifying an optimum device length.

Using a control signal with only a 10 dB *ER* instead of 20 dB, a power of 21 dBm gave the same maximum *ER* that was obtained with a 14

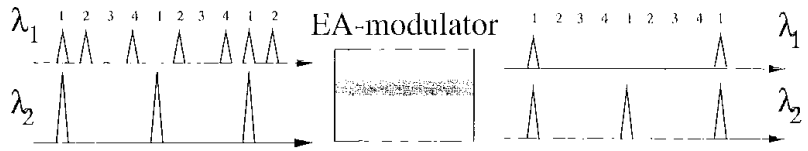

CWK70 Fig. 1. The demultiplexing configuration: Here an incoming signal at λ_1 and a local control signal at λ_2 are launched into an electroabsorption modulator. At the output, the signal aligned with the control signal is demultiplexed, the other three channels are rejected.

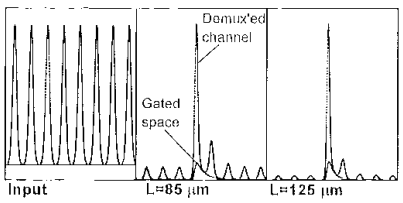

CWK70 Fig. 2. Eye diagrams of all 8 OTDM channels at the output as function of device length. At the input, all channels are equal, but into the device, other channels than the demultiplexed are rejected. The time window is 100 ps. The control pulse energy was 14 dBm, and the average OTDM pulse power was 7 dBm.

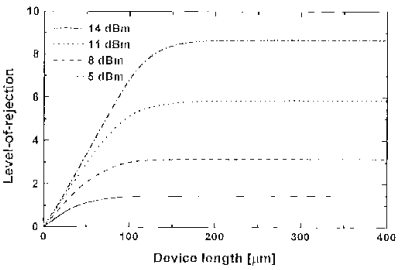

CWK70 Fig. 3. Level-of-rejection as function of length with average control pulse power as parameter. The level-of-rejection, determined by one of the rejected channels or by the gated space (whichever gives the worst eye), levels out when the control pulses become too weak to saturate the device, but the signal levels keep decreasing. Bit-patterns were chosen to obtain the greatest possible impairment.

dBm control signal with a 20 dB *ER* (Fig. 3), but for a longer device of 210 μm.

In summary, we have modeled all-optical demultiplexing using an electroabsorption modulator, and shown critical dependence of the level-of-rejection on device length and control signal power. The device is very simple, and suitable for demultiplexing OTDM signals.

1. A.D. Ellis, J.K. Lucek, D. Pitcher, D.G. Moodie, D. Cotter, "Full 10 × 10 Gbit/s OTDM data generation and demultiplexing using electroabsorption modulators," Electron. Lett., **34**, (18) 1766–1767 (1998).
2. N. Edagawa, M. Suzuki, S. Yamamoto, "Novel wavelength converter using an electroabsorption modulator: conversion experiments at up to 40 Gbit/s," in Tech. Dig. OFC'97, 1997, vol. 6 of 1997 Technical Digest Series, pp. 77–78.
3. N. Edagawa, M. Suzuki, S. Yamamoto, "Novel Wavelength Converter Using an Electroabsorption Modulator," IEICE Trans. Electron., **E81-C**, (8) 1251–1257 (1998).
4. H. Kurita, I. Ogura, H. Yokoyama, "Ultrafast All-Optical Signal Processing with Mode-Locked Semiconductor Lasers," IEICE Trans. Electron., **E81-C**, (2) 129–139 (1998).
5. H. Yokoyama, Y. Hashimoto, H. Kurita, "Noise reduction in optical pulses and bit-error-rate improvement with a semiconductor-waveguide saturable absorber," in Tech. Dig. CLEO'98, 1998, vol. 6 of 1998 Technical Digest Series, pp. 502–503.
6. S. Højfeldt, S. Bischoff, J. Mørk, "All-optical wavelength conversion and signal regeneration using an electroabsorption modulator," in Tech. Dig. LEOS'99, 1999.

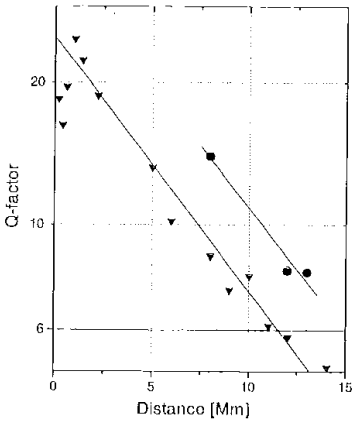

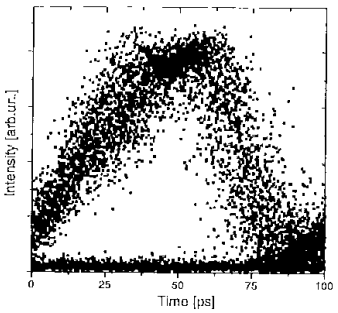

CWK71 Fig. 1. Q-factor dependence on distance for 1311 nm (triangles) and 1308.6 nm (circles). Typical eye diagram for 8 000 km distance.

CWK71

Long-haul soliton transmission in a standard fiber at 1.3 μm with distributed Raman amplification

A. Okhrimchuk, G. Onishchukov, F. Lederer, *Inst für Angewante Physik, Friedrich-Schiller Univ. Jena, Max-Wien-Platz 1, D-07743 Jena, Germany; E-mail: okhrim@iap.uni-jena.de, photonics@iap.uni-jena.de*

The desired increase of transmission capacity demands to develop optical amplifiers for the expanded optical communication window 1.3–1.6 μm. Raman fiber amplifiers are among the most promising candidates to achieve this goal because of their flexibility regarding the operation wavelength, i.e., only a pump source with an appropriate wavelength is necessary. Broadband Raman amplifiers and Raman amplifiers as supplement to EDFAs have attracted a considerable deal of interest in recent years,[1,2] but beyond 1.5–1.6 μm communication window the long-haul transmission with Raman amplification are not investigated yet. In this work we report on a transmission experiment over 10,000 km with distributed Raman amplification in 1.3 μm region.

We have investigated 10 Gb/s soliton propagation in the 1.3 μm wavelength region using a re-circulating fiber loop set up. Distributed Raman amplification in a *standard communication fiber* was used to compensate for losses in the 24 km fiber and 5 dB losses in additional elements (3.1 nm optical bandpass filter, acousto-optical switch, 20% coupler, isolators). The counter-propagating pump scheme was chosen. The pump source was a 1.24 μm cascaded fiber Raman laser pumped by an 1.06 μm Yb-doped fiber laser. In order to stabilize the Raman gain, the laser diode current in the Yb laser was controlled by the 1.24 μm output of the Raman laser through electro-optical feedback. An intensity modulator governed by a random pulse generator was used to convert the optical pulses from an external cavity mode-locked semiconductor laser to the PRBS format.

We have obtained error free-propagation ($Q > 6$) up to 10 000 km at 1307–1311 nm wavelengths in a fiber with zero dispersion at 1305.3 nm. No stable propagation has been achieved at zero dispersion wavelength and in normal dispersion domain. For anomalous group velocity dispersion it has been found that the Q-factor strongly depends on the pulse energy, and the optimum energy is found to be the fundamental soliton energy. This optimum pulse energy is proportional to the fiber dispersion in the 1305.3–1306 nm range as for solitons with a fixed duration. The propagation near zero dispersion wavelength was poor because of low soliton energy and consequently low signal to noise ratio. The best results were obtained near 1308 nm. Non-transform limited 20 ps input pulses are narrowed down to 5 ps as a result of transformation into solitons during a few hundred km. The dependence of the Q-factor on the distance near the optimum wavelength and a typical eye-diagram are shown in Fig. 1.

We have found that timing jitter and not the signal to noise ratio degradation is the main limiting factor for long distance transmission in such a system. The measured dependence of